An Electrochemical Biosensor based on Nucleic Acids Enzyme and Nanochannels for Detecting Copper (II) ion

Wentao Xu, Longjiao Zhu, Xiangli Shao, Kunlun Huang, Yunbo Luo

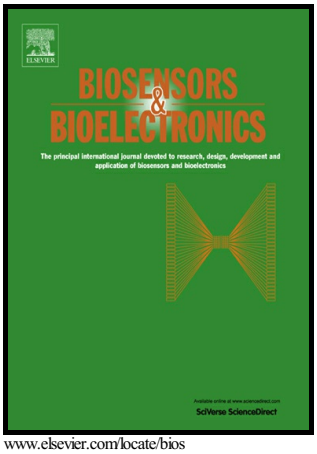

www.elsevier.com/locate/bios

PII: S0956-5663(18)30627-4
DOI: https://doi.org/10.1016/j.bios.2018.08.033
Reference: BIOS10697

To appear in: *Biosensors and Bioelectronic*

Received date: 22 June 2018
Revised date: 11 August 2018
Accepted date: 13 August 2018

Cite this article as: Wentao Xu, Longjiao Zhu, Xiangli Shao, Kunlun Huang and Yunbo Luo, An Electrochemical Biosensor based on Nucleic Acids Enzyme and Nanochannels for Detecting Copper (II) ion, *Biosensors and Bioelectronic,* https://doi.org/10.1016/j.bios.2018.08.033

An Electrochemical Biosensor based on Nucleic Acids Enzyme and Nanochannels for Detecting Copper (II) ion

Wentao Xu, [a,b,c] Longjiao Zhu,[a,b] Xiangli Shao, [a,b] Kunlun Huang, [a,b,c,*] Yunbo Luo,[a,b,*]

[a] Beijing Advanced Innovation Center for Food Nutrition and Human Health, College of Food Science & Nutritional Engineering, China Agricultural University, Beijing, 100083, China

[b] Key Laboratory of Safety Assessment of Genetically Modified Organism (Food Safety), Ministry of Agriculture, P.R. China, Beijing, 100083, China

[c]Beijing laboratory for food quality and safety, college of food science and nutritional engineering, china agricultural university, beijing 100083, China

foodsafety66@cau.edu.cn (Kunlun Huang)

lyb@cau.edu.cn (Yunbo Luo)

[*]**Corresponding Author**

Abstract:

An electrochemical biosensor based on Cu^{2+}-dependent cleavage DNAzyme (cDNAzyme), Exponential Amplification Reaction (EXPAR), and single-strand triggered DNA hybridization chain reaction (HCR) was developed for detecting the copper (II) ions. This method capitalizes on the specific recognition of cDNAzyme, the single strand accumulated isothermal amplification of EXPAR, and the enzyme-free isothermal DNA assembly of HCR. In the presence of Cu^{2+}, the catalytic chain of cDNAzyme split the substrate chain to produce single-stranded DNA (Oligo X). With the help of the EXPAR, the trace Oligo X was amplified and converted to initiator DNA (Oligo Y). After adding the initiator DNA (Oligo Y) into nanochannel, massive DNA superstructures grew from the capture probe (CP) that were pre-immobilized on the nanochannel wall, resulting in a sharp decrease of the effective diameter of the nanochannel. As a result, the transmembrane ionic current significantly decreased due to the effective closing of the nanochannel. Finally, the copper (II) ion was detected by monitoring the changes of transmembrane ionic current. The developed electrochemical biosensor also displayed high selectivity for Cu^{2+}, which could be useful for monitoring Cu^{2+} above ten picomole.

Keywords: Copper (II) ions, cleavage DNAzyme, Exponential Amplification Reaction, Hybridization chain reaction, nanochannel, electrochemical biosensor.

1.Introduction

Copper (II) ion (Cu^{2+}), the most essential transition metal ion in the human body, is responsible for myriad physiological functions(Liu et al. 2014). However, an excess dose or accumulation of copper is highly toxic to the human body and can result in issues such as liver or kidney damage(Festa and Thiele 2011), gastrointestinal disturbance, Parkinson's disease(Barnham and Bush 2008), and Alzheimer's disease(Mihai et al. 2015). Cu^{2+} contamination has been reported in many locations, earning it a spot on the Environmental Protection Agency's (EPA) list of priority pollutants(Regulations 1991).

In order to measure Cu^{2+} levels and control Cu^{2+} pollution, as well as its toxic effects, scientists developed various analytical techniques and methods, including fluorescence spectrometry(Chaiyo et al. 2013), inductively coupled plasma mass spectrometry (ICP-MS), inductively coupled plasma atomic emission spectrometry (ICP-OES)(Atanassova et al. 1998; Zhu et al. 2009) and atomic absorption spectrometry (AAS)(Pourreza and Hoveizavi 2005). However, these traditional methods required sophisticated equipment and complicated procedures for analyzing copper (II) ions, hindering their accessibility and application. Alternatively, fluorescent chemosensors for heavy metal ions using inexpensive equipment and selective chemical probe had been reported, such as QDs-based (Wang et al. 2011), carbon nanodots based(Liu et al. 2014) and sugar–rhodamine based fluorescent sensor (Yin et al. 2013), because fluorescence measurements are usually very sensitive. Although the fluorescence sensor is relatively simple and sensitive, the chemical regents is not environment friendly, the nanomaterial is required sophisticated surface modification and the fluorescence signal is easily affected by many factors such as the measurement environment. As a result, a simple, reliable, sensitive, and green strategy based on environment-friendly and reliable nanomaterials for Cu^{2+} detection was urgently needed.

The versatile structural & functional, easily synthesized, highly stabile, cost-effective and environment-friendly properties make DNA an exciting and programable material for nanotechnology, material science and bioanalysis. The nucleic acids enzyme (NAE), one type of functional nucleic acid, demonstrates strong metal ion-dependent cleavage activity for various metal ions, such as $Cu^{2+,}$(Carmi et al. 1998; Carmi and Breaker 2001), $Pb^{2+,}$(Li et al. 2014; Pelossof et al. 2012), $Mg^{2+,}$(Yuan et al. 2007), $Zn^{2+,}$(Lu et al. 2012; Nelson et al. 2005) and $UO_2^{2+,}$(Lee et al. 2008). All NAEs consist of two strands: the enzyme strand and the substrate strand. In the presence of a target metal ion, cleavage activity of enzyme strand was activated and the substrate strand was cleaved into two single strands (Zhou et al. 2017). The metal ion-dependent cleavage activity make NAEs convenient tools to transfer metal ion targets into nucleic acid targets for further nucleic acid based signal amplification(Zhu et al. 2017a) or nanomaterial based signal output(Liu and Lu 2005). Recently, the isothermal amplification strategies were very popular for nucleic acid amplification due to they can perform in an constant temperature using a simple water bath or heating block (Ikbal et al. 2015). Dirks and Pierce first reported an hairpin-assisted and initiator-catalyzed DNA self-assembly strategy, in which two metastable hairpins will switch on a fabricate reaction of long-nicked super dsDNA nanostructures upon the addition of initiator DNA (Target DNA), called hybridization chain reaction (HCR) (Dirks and Pierce 2004) . Due to the outstanding properties in DNA isothermal and enzyme-free assembly, it

has been applied in many biosensors for analysis of various targets. For example, Ling group reported an ultrasensitive electrochemical sensor for Hg^{2+} by using HCR coupled with Ag@Au core–shell nanoparticles (Li et al.2016). Zhang group fabricated homogeneous bioluminescence sensor of biomolecules using target-triggered HCR-mediated ligation without luciferase label (Xu et al.2013). Tang group reported a cyclometalated iridium complex-based label-free photoelectrochemical biosensor for DNA detection by HCR (Li et al.2015). To further enhance the sensitivity, the two-step amplification strategy combination of HCR with other isothermal amplification method was urgently need. Exponential Amplification Reaction (EXPAR) is an ideal isothermal amplification strategy for coupling with HCR because its single strand DNA accumulation capability (Ness et al. 2003). The EXPAR can be specifically triggered by the given single-strand sequence and used to amplify small amounts of the given oligonucleotides to 10^6-10^9-fold in less than 20 minutes under isothermal conditions using a combination of polymerase strand extension and single-strand nicking(Van Ness et al. 2003). The accumulated short single-strand oligonucleotides could be customized setting by rationally designing the sequence of amplification template(Jia et al. 2014). EXPAR's high amplification efficiency, powerful isothermal amplification, and overall design make it an important tool to bridge the cDNAzyme recognition platform with HCR amplification platform by enriching the single strand oligonucleotides (the cleaved single strand from cDNAzyme) into specified DNA sequences (the initiator DNA of HCR).

The gating of biological nanochannels is the basis signal-transduction processes in cell (Reisner et al.,2012). The gating process is generally activated by molecular stimuli by moving the nanochannel between opened and closed states. Inspired by the interesting gating process in living organisms, some research group developed artificial nanofluidic gating systems based on the synthetic, solid state nanochannel to perform analysis functions (Hou et al. 2011; Shang et al. 2013). This synthetic porous membrane nanochannel is more mechanically and chemically robust than the natural ion channels embedded in the lipid-bilayer membrane(Hou et al. 2009). The artificial gate-like nanofluidic devices able to perform stimuli-responsive & sensing functions have been developed by immobilizing responsive molecules onto the surface of inner wall of nanochannels (Liu et al. 2015; Zhang et al. 2013). However, the previous developed gating system were suffered from poor sensitivity because one molecular target specifically combined with one signal probe producing just one share of signal increment. And the types of analytes were also limited by the specific modified capture probe, such as antibody, chemical receptor. Thus, we firstly planted the artificial nanochannel with our designed cDNAzyme &EXPAR-assisted HCR DNA assembly system to improve the sensitivity and generality of nanofluidic gating sensor.

In this study, we reported a highly efficient and Cu^{2+} stimuli-responsive electrochemical biosensor that integrated a Cu^{2+}-dependent cleavage DNAzyme for target recognition and transformation with EXPAR-assisted HCR for two step signal amplification and a solid state nanochannel for signal readout. The constructed electrochemical biosensor for Cu^{2+} was performed in a wild way under the isothermal condition. Quantitative detection is easily achieved by determining On-off ratio change based on ionic current variation. More importantly, the fabricated sensing system has the potential to detect various

targets simply by adjustment of the sequence of the cleavage DNAzyme and EXPAR's template. Our nanofluidic gating system based electrochemical biosensor offers an environment-friendly and ultrasensitive approach for monitoring metal ions.

2.Material and methods

2.1. Reagents and Apparatus

The nanoporous alumina membranes were purchased from PuYuan Nano (Hefei, China). (3-aminopropyl) trimethoxysilane (APS,97%) was purchased from sigma. Glutaraldehyde solution (25% in H_2O) and Tris (hydroxymethyl) aminomethane (Tris, 99%) were purchased from Amersco. All DNA sequences were synthesized by Kare Bay Biochem Co., Ltd. (Ningbo, China), and used as received after dissolving in water. Dynabeads® MyOne™ Streptavidin T1, 50 bp Ladder DNA marker, and SYBR Gold nucleic acid gel stain was purchased from Thermo Fisher Scientific (Life Technologies, Beijing, China). Bst DNA polymerase and Nt.BstNBI nicking endonuclease were purchased from New England Biolabs (NEB, Beijing, China). Ultrapure water (resistivity ≥ 18.2 MΩ cm^{-1}, Milli-Q system) was used. All chemical reagents were analytical grade. Gel electrophoresis was conducted on a Molecular Imager Gel Doc XR (Bio-Rad, Beijing, China). Droplet-based digital PCR analysis was conducted by QX200 Droplet Digital PCR (Bio-Rad, Beijing, China).

2.2. Immunomagnetic assisted cleavage of Cu^{2+}-Dependent DNAzyme

80 nM substrate strand and 160 nM catalyze strand were heated at 95°C for 5 min and then incubated in 50 mM HEPES buffer (pH 7.0) containing 1.5 M NaCl at 37°C for 2 h to assemble Cu^{2+}-dependent cleavage DNAzyme (cDNAzyme). Then, the streptavidin-functionalized magnetic beads (MBs), which were pre-cleared with phosphate buffered saline (PBS) (0.15 M NaCl, 10 mM K_2HPO_4, and 1 mM NaH_2PO_4, pH 7.4), were added into cDNAzyme mixtures and incubated at 25°C for 15min to immobilize cDNAzyme on the surface of beads. The excess enzyme strand and cDNAzyme was removed by rinse and magnetic separation. Different concentrations of Cu^{2+} ($CuSO_4$, 100 μL) dissolved in the cleavage buffer (1.5 M NaCl, 50 mM HEPES and 50 μM ascorbate, pH7.0) were incubated with the MBs-cDNAzyme complex at 37°C for 1 h. An equal volume of cleavage mixture without Cu^{2+} was used as the negative control. Then, magnetic separation was implemented to separate the single strand cleaved Oligo X.

2.3. The characterization of cDNAzyme cleavage by Digital PCR

The droplet-based digital PCR (ddPCR) reaction system (Zhu et al. 2017b) contained 1×ddPCR Master Mix, 0.24 μM forward primer, 0.24 μM reverse primer, 0.12 μM Taq Man probe and 2 μL of the Cu^{2+}-dependent DNAzyme cleavage product in a 20 μL reaction volume. In contrast, 2 μL Cu^{2+}-dependent DNAzyme solution was added as the negative control. This mixture was transferred to a disposable eight-channel droplet generator cartridge. In total, 70 μL droplet generation oil was loaded to each well. After the droplet generation step and PCR amplification, the PCR products were analyzed in the droplet-reading step. Each droplet was analyzed by the beta-prototype droplet reader. The fluorescence of each droplet was also measured.

The PCR amplification procedure, used in this section, consisted of a denaturation step at 95°C for 5 min, 50 cycles of a two-step thermal profile with 10 s at 95°C for denaturation and 60 s at 60°C for extension. Finally, a 95°C step for 5 min was conducted to stabilize the droplet.

2.4. EXPAR for accumulation of single strand Oligo Y

EXPAR assays were performed in a 32.5 μL total reaction mixture. 6 μL 1uM X'-Y' template, 3 μL 2.5 mM dNTP, 6 μL signal precursor Oligo X and 9 μL ultrapure water were first mixed together and incubated at 95 °C for 5 min. Then 0.1 μL 8 U/μL Bst DNA polymerase and 3 μL 10×thermopol buffer, 1.8 μL trehalose, and 0.9 μL BSA were added into the mixture and incubated at 55°C, 10 min. Finally, 1.2 μL Nt.BstNBI nicking endonuclease and 1.5 μL 1×Nt.Bst NBI reaction buffer (buffer 3.1) were added in the mixture and incubated at 55°C for 20 min. After the amplification reaction, the single-stranded product (Oligo Y) was purified by magnetic separation. The amplification effect of EXPAR was characterized by non-denaturing 20% PAGE (Table S1).

2.5. Fabrication of smart gating system

Chemical modification of nanochannel. Nanoporous alumina membranes were thoroughly cleaned in absolute ethyl alcohol for 15min using an ultrasonic method. Then, the membranes were immersed in 5% HCl solution for 30 s to expose the hydroxy group. After being thoroughly washed in distilled water and dried, the membrane was added into a 5% acetone solution of 3-aminopropyltrimethoxysilane (APS) and incubated at 28°C for 2 h. The membranes were then thoroughly washed and dried at 70°C for 2 h to immobilize the amino group. Finally, the membranes were immersed in a 25% aqueous solution of glutaraldehyde overnight to immobilized the aldehyde group (Vlassiouk et al. 2004).

Single strand Oligo Y triggered DNA assembly via HCR. The capture probe was immobilized on the channel wall by immersing the membranes in a 10 mM Tris-HCl buffer (containing 500 mM NaCl, 1 mM $MgCl_2$, pH=7.4) with 1 μM 5'-aminated capture DNA for 6 h. For DNA assembly, the membranes were washed with distilled water and incubated with the purified EXPAR product for 3 h. Then, the membranes were rinsed with water and immersed in 1 mL HCR buffer (2.5 mM NaH_2PO_4, 8 mM Na_2HPO_4, 0.15 M NaCl, and 2 mM $MgCl_2$, pH 7.4) containing 1 μM H1 and 1 μM H2 overnight at room temperature.

2.6. Characterization of DNA assembly and Current–Voltage Recording

The Scanning Electron Microscope (SEM) (Phenom Pro) and Laser Scan Confocal Measurement (LSCM) (Nikon Eclipse T*i*) confirmed the formation of DNA assembly on the membrane surface and inside the nanochannel, respectively. Notably, the LSCM should be assisted by the fluorescence labeling. The transmembrane ionic current was measured by Ag/AgCl electrodes. To measure the transmembrane ionic current, the nanoporous alumina membrane was mounted between two PMMA cells, and the electrolyte solution was 1 mM KCl. The transmembrane potential was determined by the Keithley 2636B picoammeter/voltage source (Keithley Instruments) through Ag/AgCl electrodes.

3.Results and Discussion

3.1. Principle of smart nanofluidic gating system based biosensor for Cu^{2+}

The copper (II) ion stimuli-responsive nanofluidic gating system was fabricated based on three working platforms (A, B and C). A detailed schema of each working platform is illustrated in Figure 1.

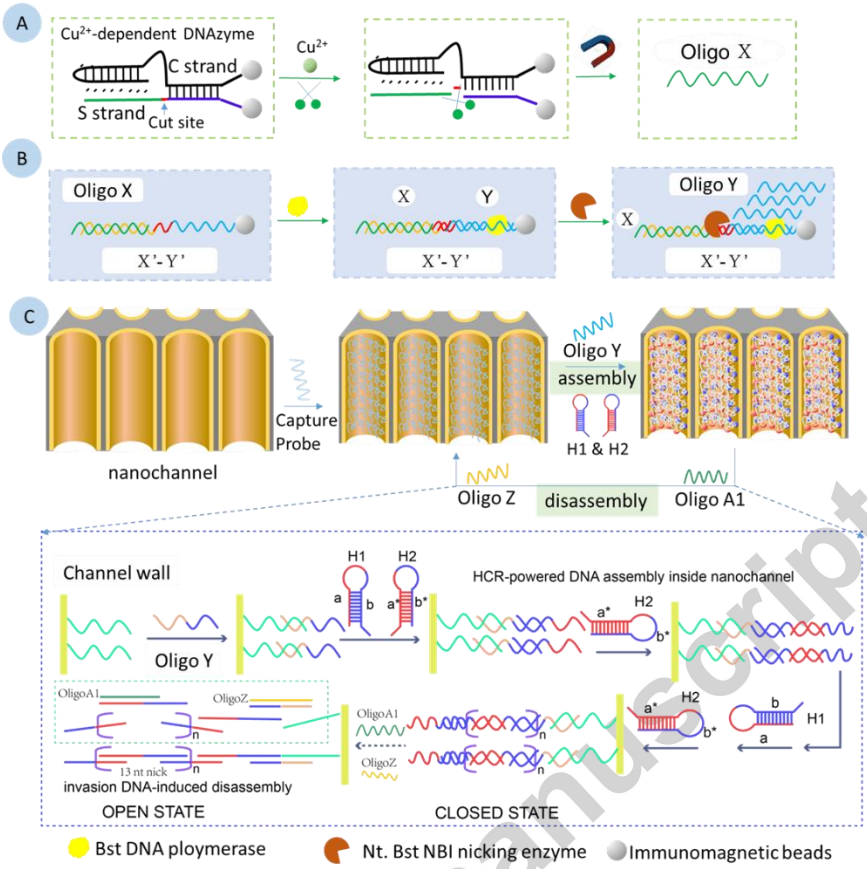

Figure 1. The principle of Cu^{2+} stimuli-responsive electrochemical biosensor. (A) The cDNAzyme assisted target transformation platform. (B) The EXPAR assisted signal Oligo Y enrichment platform. (C) The Oligo Y triggered and HCR assembly powered nanofluidic gating system.

In the working platform A, the non-nucleic acid target Cu^{2+} was transformed into a single strand nucleic acid, termed signal precursor oligonucleotides X (Oligo X). Firstly, the biotinylated substrate strand (S strand) and catalyze strand (C strand) were assembled into cDNAzyme. Subsequently, the cDNAzyme was immobilized on the MBs via the streptavidin-biotin bridge system. In the presence of Cu^{2+}, the cleavage activity of cDNAzyme was activated, resulting the substrate strand cleaving into short single-stranded Oligo X. After magnetic separation, the Oligo X was purified from the cleavage products. It is worth noting that the transformation of the target in platform A was linear and the converted Oligo X was a specific sequence. To enhance the sensitivity and detection throughput, we enriched the specific signal precursor Oligo X to a general signal Oligo Y via EXPAR.

Platform B schematically illustrates the enrichment and transformation of Oligo X. Firstly, EXPAR enables Oligo X to hybridize with template X'-Y' as a primer to initiate the strand extension along the template with the help of Bst DNA polymerase and deoxyribonucleotide trisphosphates (dNTPs). The nicking endonuclease Nt.BstNBI recognized the cutting site (red highlight in Table S2), which was located in the middle of the double-strand products X-Y. The cleaved X strand continued extended via DNA polymerase and the cleaved OligoY peeled off from template X'-Y' via the

strand-displacement reaction. As a result, the extension, cleavage, and strand displacement were in circulation for exponential accumulation of general signal Oligo Y under an isothermal condition. After platform B, the accumulated signals of Oligo Y were purified by magnetic separation.

Finally, the Oligo Y triggered the hairpin-assisted DNA assembly via HCR in nanochannels, generating a nanofluidic gating system. In this platform, the aminated capture probe (CP) was pre-immobilized on the nanochannel wall via chemical modification. Then Oligo Y was added, half of Oligo Y was complementary with CP, the remained half first hybridize with the 'sticky end' of H1, then hybridize with section 'b' of H1 via strand displacement. H1 was opened and released section 'a' to open H2 to form complex I-H1-H2 containing single-stranded segment "b*", which continuously mediate a branch migration by means of base-pairing. As a result, a DNA superstructure grew from the Oligo Y and stuffed the nanochannel (CLOSED state). The effective pore size of nanochannel sharply decreased, leading a significant reduction of the transmembrane ionic current. In the absence of Cu^{2+}, each platform was not work. The nanochannels remained in the OPEN state, the transmembrane ionic current was significantly higher. In this paper, the copper (II) ion was measured via monitoring the changes of transmembrane ionic current. The sequences used to fabricate the nanofluidic gating could be found in Table S2.

3.2. Characterization of cDNAzyme cleavage by digital PCR

The droplet-based digital PCR (ddPCR) analysis was performed to demonstrate the cleavage activity of Cu^{2+}-dependent cleavage DNAzyme. By adding primer-combination sequences to the two flanks of the substrate strand of cDNAzyme (Table S3), the cleaved cDNAzyme could not be amplified by Polymerase Chain Reaction (PCR). This inability to amplify was due to the breakage of the template strand, which was not a challenge faced by the integrated cDNAzyme. The hot map of digital PCR amplification is shown in Figure 2. The pink line represents the fluorescence threshold. Blue dots above the pink line represent the positive amplification of droplet samples, which indicate the uncut cDNAzyme. Gray dots below the pink line represent the negative amplification of droplet samples, which indicate the cleaved cDNAzyme. In Figure 2A, the abundance of blue dots clustered above the pink line, as well as the scarcity of gray dots aggregated below this line, demonstrate the integrity of Cu^{2+}-dependent DNAzyme. In contrast, in Figure 2B, a plentiful number of gray dots clustered below the pink line while few blue dots accumulated below, indicating the cleavage of the cDNAzyme. The sequence used in this section was listed in Table S3.

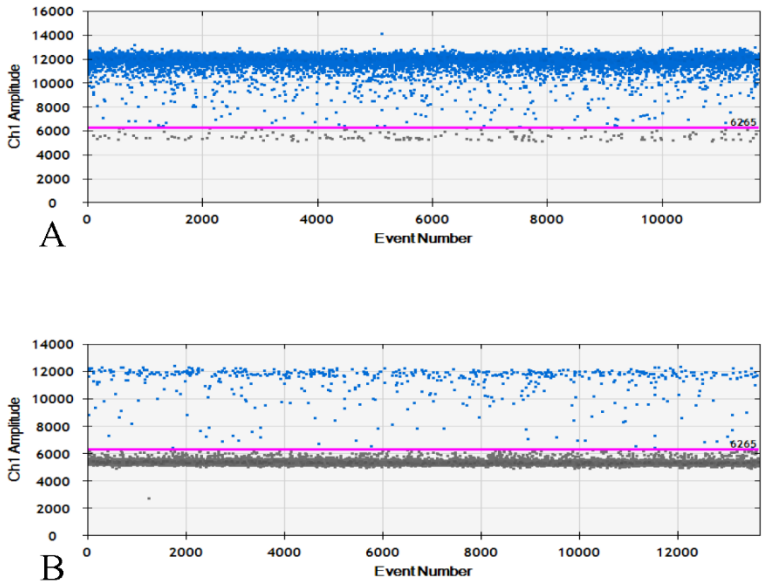

Figure 2. Droplet-based digital PCR analysis demonstrating the cleavage activity of Cu^{2+}-dependent cleavage DNAzyme. Hot map of ddPCR (A) without Cu^{2+} or (B) with 80 nM Cu^{2+}.

3.3. Amplification Effect of EXPAR

EXPAR's amplification effects were detected by non-denaturing 20% PAGE, as well as fluorescent detection with SYBR gold dye. As shown in Figure 3A, compared with the negative control in lane 3, the sample with Oligo X in lane 1 produced many single-stranded Oligo Y (black arrow), which correspond with the band of positive control in lane 2. The smears shown in lane 1 below the bands of Oligo Y further confirmed the dynamic strand displacement reaction during the EXPAR. We continue monitor the signal strand in each sample by fluorescent quantitation. After EXPAR, the positive samples have dramatically more pronounced fluorescent signals than the negative control (2.5-fold), demonstrating the production of plentiful single-stranded Oligo Y. We further quantified the Oligo Y via the calculation of P (positive) /N (Normal) ratio between the positive sample and positive control. The detailed calculation was as follow:

P/N ratio= (positive sample-negative control) fluorescent intensity/positive control fluorescent intensity

After calculation, the P/N ratio was 1.2. Finally, we can determine that the positive sample contained approximately 2.4 μM.

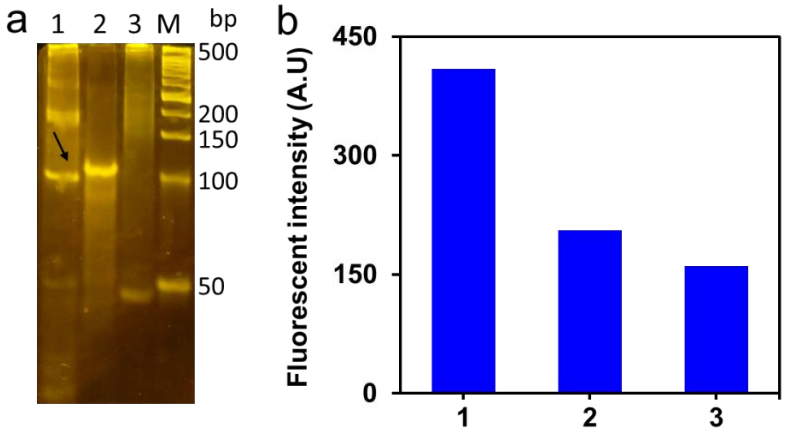

Figure 3. The amplification effect of EXPAR. (a) non-denaturing 20% PAGE of EXPAR; (b) Quantitative fluorescent analysis of EXPAR with SYBR Gold. (1) positive sample: the EXPAR condition with 1 μM Oligo X. (2) positive control: 2 μM oligo Y. (3) negative control: the EXPAR condition with 0 μM Oligo X.

3.4. Characterization of DNA assembly in nanochannel

The Laser Scanning Confocal Microscopic (LSCM) measurement was used to monitor the condition of HCR-powered DNA assembly inside the nanochannels. The dashed line in the picture (a)&(b) indicates the membrane surface. Assisted by the fluorescence label of hairpins, we observed that the strong fluorescence filled with the nanochannel and the thickness of cross-section fluorescence was approximately the same thickness of the nanoporous alumina membranes (Figure 4b). The observed cross-section fluorescence proved that the Oligo Y successfully triggered the HCR-powered DNA assembly inside the nanochannels and stuffed in nanochannels. However, after adding fluorescent labeled Hairpins, the nanochannel have not been observed with any fluorescence in absence of Oligo Y (Figure 4a). This further proved that Oligo Y was necessary for HCR-powered DNA assembly inside the nanochannels.

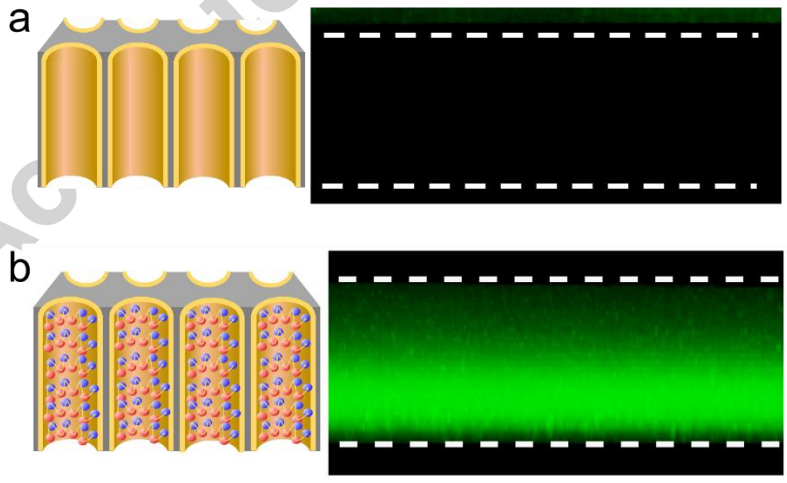

Figure 4. The LSCM characterization of HCR-powered DNA assembly inside the nanochannels (a) without addition of Oligo Y and (b) with addition of Oligo Y.

3.5. The DNA assembly induced variation of transmembrane ionic current

The significant change in membrane surface topology, as well as the channel size change inside the nanochannel (caused by the Oligo Y-triggered DNA assembly), leading to a highly efficient and responsive nanofluidic gating system. After modification with the capture probes (red circle group, Figure 5), the transmembrane ionic current remained in the OPEN state and was 9.23×10^{-6} A. In absence of Oligo Y, only a very limited reduction in the transmembrane ionic current was found, even with the presence of H1 and H2 (black square, Figure 5). In contrast, in the presence of Oligo Y, the ionic current fell sharply from 9.23×10^{-6} A (the ON state) to the 4.74×10^{-10} A (the OFF state, blue triangle, Figure 5). The measurement voltage was +2 V, and the On-Off ratio approached 1.67×10^{4}. The On-Off ratio in this paper was higher than the previously reported chemically modified gating system (Abelow et al. 2010; Schepelina and Zharov 2007). The high gating efficiency of the transmembrane ionic current stems from the greatly improved steric hindrance of DNA assembly. Further, the flexible nature of DNA assembly also makes DNA liable to fill up the nanochannel more than other "hard" nanoscale building material, resulting in a high gating efficiency.

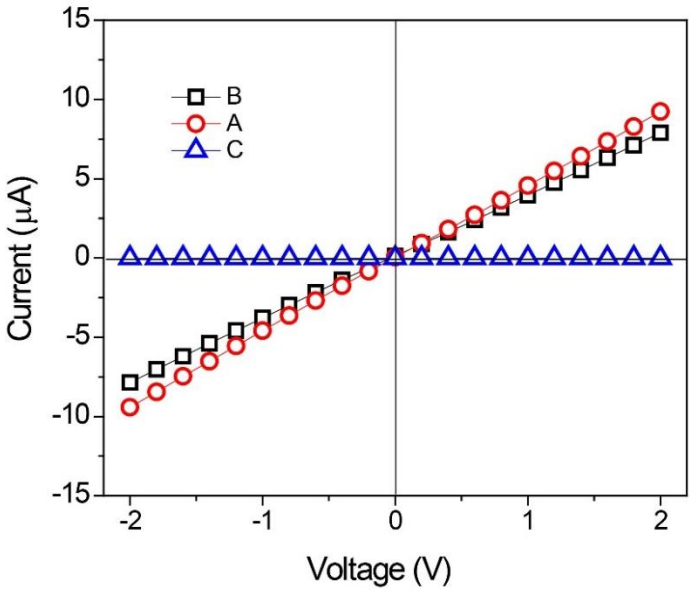

Figure 5. The comparison of transmembrane ionic current with different DNA probe modification. (A) red circle group, the membrane modified with capture probe only. (B) black square group, the membrane modified with capture probe, H1 and H2. (C) Blue triangle group, the membrane modified with capture probe, Oligo Y, H1 and H2.

3.6. The analytical performance of smart gating system-based biosensor

The fabricated biosensor can achieve quantitative response to copper (II) ions. We applied a series of concentrations of converted Oligo Y to stimulate the nanochannel. From the I-V curves (Figure 6a), we can see that the smart nanofluidic gating system can sensitively respond to copper (II) ions above 10 picomole. However, a limited reduction of ionic current was observed when the concentration of copper (II) ions was below 10 picomole. The United States Environmental Protection Agency (EPA) permits a maximum level of Cu^{2+} in drinking water of 20 μM (Liu and Lu 2007) – the detection limit is much lower. For quantitative analysis, the binomial equation $y = 882.39x2 - 2727.9x + 1870.1$, $R^2 = 0.965$ could be used.

The specificity of smart nanofluidic system was evaluated by testing other metal ions, including Pb^{2+}, Hg^{2+}, and Ag^{+}, as well as mixed ions. As Figure 6b illustrates, the smart gating system shows a

negligible On-Off ratio for interfering metal ions. The results indicated that the fabricated biosensor exhibits excellent specificity toward Cu^{2+}.

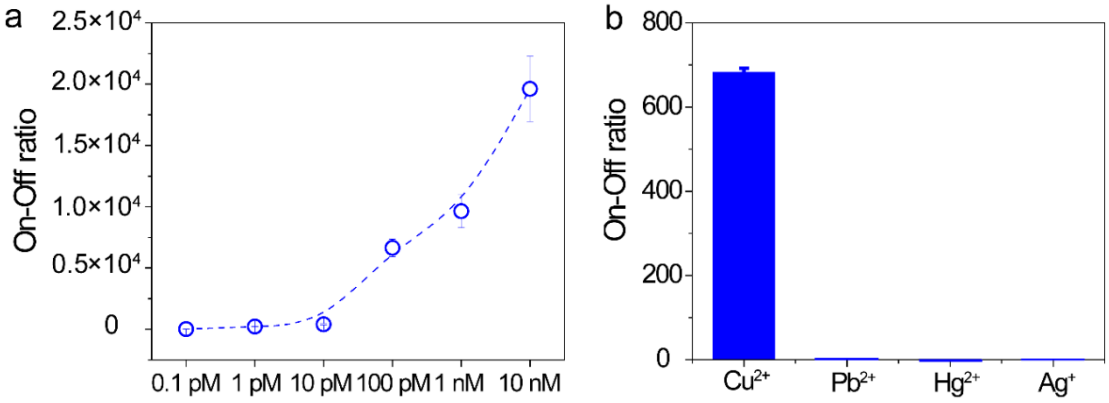

Figure 6. Analytical performance of the fabricated biosensor. (a)The concentration response and (b) the specificity of the smart nanofluidic gating system-based biosensor.

In addition, the reproducibility of method was studied using 8 group of electrochemical biosensors which prepared under the same conditions on different days. A relative standard deviation (RSD) of 9.88 % for 100 pM Cu^{2+} was obtained, indicating the satisfied inter-biosensor reproducibility of the resulting electrochemical biosensor for practical application. And to measure the reproducibility of the equipment (Keithley 2636B picoammeter/voltage source), a set of 6 successive ionic current measurements for 100 pM copper (II) ion using same electrochemical biosensor yield an RSD of 4.26%, showing that the equipment was stable and the good intra-biosensor reproducibility. The detailed information was listed in table S5-6.

The storage stability of the biosensor was tested for 4 weeks. The nucleic acids functionalized nanochannels was stored at 4°C before testing and was detected weekly. In the first week, approximately 16.66 % of the On-Off ratio was lost, indicating the good storage stability for the sensor. After 2nd-3rd weeks, 32.92 % and 34.09 % of its initial response was declined, indicating the weak storage stability for the sensor. After 4th weeks, the On-off ratio remained 8% of its initial response, indicating the poor storage stability for the sensor. The weak storage stability maybe attributed to that nucleic acids cannot storage at 4°C for a long time. Therefore, the functionalized nanochannel shouldn't been storage for a long time before use. The detailed information was listed in table S7.

3.7. The reversibility of the smart gating system

To achieve cyclic utilization of the functional nanochannel, we firstly designed an invasion DNA (Oligo Z) to remove the DNA assembly form the nanochannel wall by strand displacement. We valued the disassembly capacity of Oligo Z by measuring the ionic conductance. After incubation with the Oligo Z for 6 h, the DNA assembly modified nanochannel had not demonstrated an increase of ionic conductance. From the fluorescent image shown in Figure S2, one can see that, even after invasion DNA treatment, residual DNA assembly persisted in the nanochannels. Two reasons may account for the failure of disassembly. Firstly, the stripped DNA assembly remained in big-bulk nanostructure, which would be difficult to pass through the nanochannel. Secondly, the stripped big-bulk DNA assembly plugged inside the nanochannel may result in high steric hindrance that prevents Oligo Z from accessing the center of the nanochannel. As a result, the nanochannel remained in the CLOSED state. Based on these conditions, we designed an auxiliary invasion DNA (Oligo A1) to assist the

disassembly process. The Oligo A1 partially complementary with Hairpin 1 (Figure S3) to crush the DNA assembly directly by strand displacement. Then we determined the reversibility of the fabricated smart gating by circular exposure of the device to Oligo Y initiated DNA assembly and invasion DNA (Oligo A1 & Oligo Z) mediated disassembly. The ionic current measurements showed that the device could be reversibly switched between CLOSED and OPEN states for use in recycling (Figure S5). The gating efficiency remained high in the first 3 cycles. However, the devices show a remarkable decline in the gating efficiency in the subsequent cycles. The invalidation of the nanofluidic gating device may attributed to the decreased stability of immobilized capture DNA during the long-time of the experiment period.

4. Conclusion

In summary, this study demonstrated an electrochemical biosensor based on cDNAzyme and EXPAR-HCR isothermal amplification assisted smart nanofluidic gating system that can control the ionic current to response copper ion (II) stimuli. The fabricated biosensor was composed of three platforms, including the Cu^{2+}-dependent cleavage DNAzyme assisted target transformation platform, the EXPAR assisted signal enrichment platform, and the HCR assembly-powered nanofluidic gating platform. The cDNAzyme was used for the guarantee of specificity and the isothermal amplification methods EXPAR and HCR were used for the improvement of sensitivity. The nanofluidic gating system of Cu^{2+} exhibited an estimated LOD of about 10 picomole with high selectivity. It should be mentioned that two invasion DNAs (Oligo Z and Oligo A1) were successfully designed to crush the DNA assembly inside the nanochannel for cyclic utilization of the functional nanochannel. However, the storage stability and high throughput detection remained challenge problems in our present work. In the future, we should pay more attention on exploring robust artificial nucleic acids probes in order to develop more robust and practical long shelf life electrochemical analysis array for monitoring various metal ions simultaneously.

ASSOCIATED CONTENT

Supporting Information

1.Polyacrylamide Gel Electrophoresis**;** 2. The DNA sequences used in this paper**;** 3. Characterization of DNA assembly inside nanochannel; 4. Invasion DNA mediated disassembly;5.The reversibility of the smart gating; 6. Comparison with other DNAzyme based biosensor; 7. The reproducibility and stability. Additional information as noted in the text. This material is available free of charge via the Internet at http://pubs.acs.org.

Notes

The authors declare no competing financial interests.

ACKNOWLEDGMENT

This work is financially supported by the National Natural Science Foundation of China (31671922).

Reference

Abelow, A.E., Schepelina, O., White, R.J., Vallée-Bélisle, A., Plaxco, K.W., Zharov, I., 2010. Chem Commun. 46, 7984-7986.

Atanassova, D., Stefanova, V., Russeva, E., 1998. Talanta. 47, 1237-1243.

Barnham, K.J., Bush, A.I., 2008. Curr. Opin. Chem. Biol. 12, 222-228.

Carmi, N., Balkhi, S.R., Breaker, R.R., 1998. PNAS. 95, 2233-2237.

Carmi, N., Breaker, R.R., 2001. Bioorg. Med. Chem. 9, 2589-2600.

Chaiyo, S., Chailapakul, O., Sakai, T., Teshima, N., Siangproh, W., 2013. Talanta.108, 1-6.

Dirks, R.M., Pierce, N.A., 2004. P Natl Acad Sci USA.101, 15275-15278.

Festa, R.A., Thiele, D.J., 2011. Curr. Biol. 21, R877–R883.

Hou, X., Guo, W., Jiang, L., 2011. Chem Soc Rev.40, 2385-2401.

Hou, X., Guo, W., Xia, F., Nie, F.Q., Dong, H., Tian, Y., Wen, L.P., Wang, L., Cao, L.X., Yang, Y., Xue, J.M., Song, Y.L., Wang, Y.G., Liu, D.S., Jiang, L., 2009. J. Am. Chem. Soc. 131, 7800-7805.

Ikbal, J., Lim, G.S., Gao, Z.Q., 2015. Trac-Trend Anal CH.64, 86-99.

Jia, H.X., Wang, Z.B., Wang, C.L., Chang, L.J., Li, Z.P., 2014. Rsc. Adv. 4, 9439-9444.

Lee, J.H., Wang, Z., Liu, J., Lu, Y., 2008. J. Am. Chem. Soc. 130, 14217-14226.

Li, W., Yang, Y., Chen, J., Zhang, Q., Wang, Y., Wang, F., Yu, C., 2014. Biosens. Bioelectron. 53, 245-249.

Liu, J., Lu, Y., 2005. J. Am. Chem. Soc. 127, 12677-12683.

Liu, J., Lu, Y., 2007. J. Am. Chem. Soc. 129, 9838-+.

Liu, M.Y., Zhang, H.C., Li, K., Heng, L.P., Wang, S.T., Tian, Y., Jiang, L., 2015. Adv Funct Mater 25, 421-426.

Liu, Y.S., Zhao, Y.A., Zhang, Y.Y., 2014. Sensor Actuat B-Chem 196, 647-652.

Lu, C.H., Wang, F., Willner, I., 2012. J. Am. Chem. Soc. 134, 10651-10658.

Mihai, M., Bunia, I., Doroftei, F., Varganici, C.D., Simionescu, B.C., 2015. Chem. Eur. J. 21, 5220-5230.

Nelson, K.E., Bruesehoff, P.J., Lu, Y., 2005. J. Mol. Evol. 61, 216-225.

Ness, J.V., Ness, L.K.V., Galas, D.J., 2003. PNAS.100, 4504-4509.

Pelossof, G., Ran, T.V., Willner, I., 2012. Anal. Chem. 84, 3703-3709.

Pourreza, N., Hoveizavi, R., 2005. Anal. Chim. Acta.549, 124-128.

Regulations, E., 1991. Fed Regist 56.

Schepelina, O., Zharov, I., 2007. Langmuir. 23, 12704-12709.

Shang, G.L., Fei, G.T., Xu, S.H., Yan, P., Zhang, L.D., 2013. Mater Lett 110, 156-159.

Van Ness, J., Van Ness, L.K., Galas, D.J., 2003. P. Natl. Acad. Sci. USA 100, 4504-4509.

Vlassiouk, I., Krasnoslobodtsev, A., Smirnov, S., Germann, M., 2004. Langmuir. 20, 9913-9915.

Wang, J.Z., Zhou, X.P., Ma, H.B., Tao, G.H., 2011. Spectrochim Acta A. 81, 178-183.

Yin, J.X., Ma, X., Wei, G.H., Wei, D.B., Du, Y.G., 2013. Sensor Actuat B-Chem. 177, 213-217.

Yuan, B.F., Xue, Y., Luo, M., Hao, Y.H., Tan, Z., 2007. Int. J. Biochem. Cell Biol. 39, 1119-1129.

Zhang, H.C., Tian, Y., Jiang, L., 2013. Chem Commun 49, 10048-10063.

Zhou, W.H., Saran, R., Liu, J.W., 2017. Chem. Rev. 117, 8272-8325.

Zhu, P., Shang, Y., Tian, W., Huang, K., Luo, Y., Xu, W., 2017a. Food Chem. 221, 1770-1777.

Zhu, P.Y., Shang, Y., Tian, W.Y., Huang, K.L., Luo, Y.B., Xu, W.T., 2017b. Food Chem. 221, 1770-1777.

Zhu, Y.B., Inagaki, K., Chiba, K., 2009. J. Anal. At. Spectrom. 24, 891-895.

Highlights

- An artificial gate-like biosensor for ultrasensitive detection of heavy metal ion.
- The metal-specific cleaving DNAzyme was used to guarantee the specificity of sensor.
- Exponential Amplification Reaction (EXPAR) was used to amplify the signal.
- A DNA-responsive nanochannel was fabricate using the HCR powered DNA assembly.
- Cyclic utilization of the sensor was achieved using two invasion DNAs.